Informative Potential of Eddy Current Tomography

Aleksandr Goldshtein and Evgeny Yakimov

Abstract Applicability of methods used in tomography for reconstruction of electrically conductive objects of complex structure to increase the information content of eddy current testing is evaluated based on physical modeling of the interaction of the eddy current transducer magnetic field with electrically conductive objects. Methods considered imply scanning the surface of an object using an eddy current transducer with a local test area and obtaining measurement information at different angles of mutual spatial orientation of the excitation magnetic field strength vector and the test object.

1 Introduction

Tomography is one of the most informative methods in non-destructive testing and diagnostics, which provides data on each elementary volume of the object under study.

Tomography (Greek *tomos* slice, section + *graphō* write, describe) is layer-by-layer imaging of the internal structure of an object.

The application scope includes medical tomography (as a type of medical imaging and medical diagnostics), industrial tomography (as a type of defectoscopy), and tomography of macro-objects (e.g., a significant part of the atmosphere).

With regard to the type of the physical field used, tomography can be divided into radiation, optical, ultrasonic, radio wave, and magnetic resonance imaging. Radiation imaging [1] uses high-energy electromagnetic waves with frequency exceeding 3×10^{16} Hz, optical imaging [2] uses electromagnetic waves of the visual range,

A. Goldshtein · E. Yakimov (✉)
Division for Testing and Diagnostics, National Research Tomsk Polytechnic University,
30, Lenin Avenue, Tomsk, Russia 634050
e-mail: shishkovka@mail.ru

A. Goldshtein
e-mail: algol54@yandex.ru

I. V. Minin et al. (eds.), *Progress in Material Science and Engineering*,
Studies in Systems, Decision and Control 351,
https://doi.org/10.1007/978-3-030-68103-6_1

ultrasonic imaging [3] uses ultrasonic waves, radio wave imaging [4, 5] uses ultra-high frequency electromagnetic waves, and magnetic resonance imaging [6] uses high-frequency electromagnetic waves in combination with strong constant magnetic fields.

In [5], it is shown that eddy current testing based on excitation of eddy currents in the electrically conductive parts of the test object by low-frequency magnetic fields in the range of (10^1 to 10^7) Hz can be effectively used to solve a number of tomography problems in engineering.

These methods can be used to obtain detailed data on the structure of composite metal objects. Eddy current testing is superior to other physical methods used in tomography due to high test performance, safety and ability to obtain data with one-way access to the test object (compared to radiation methods), higher penetrating power and ability to obtain data on electromagnetic properties of the object (compared to optical and radio wave methods), ability to obtain data on the object structure with gaps (compared to acoustic methods), and ability to test objects made of high electrically conductive materials (compared to magnetic resonance tomography).

Reconstruction of objects of a complex structure (design) based on the data obtained in eddy current testing is performed similarly to that used in the tomography types listed above, employing mainly two methods to increase the information content of testing.

The first method implies scanning the object surface when detecting the interaction zone of the exciting magnetic field of the eddy current transducer (ECT) and the test object.

In the second method, data are obtained at different angles of mutual spatial orientation of the field strength vector of the exciting magnetic field and the test object. In contrast to the first method, the second method employs an ECT with high uniform sensitivity to the object in the entire test area.

Thus, in terms of tomography, we can assert that ‘multi-angle’ interaction of a physical field with an object can be used to increase the information content.

We agree with the authors of the monograph [5] on the fundamental applicability of low-frequency magnetic fields for tomography of technical objects, however, we suggest the term ‘magnetic tomography’ for this type of tomography. With regard to the specifics of the physical interaction of the exciting field and the test object, it is more logical to use the term ‘eddy current tomography’. The conclusions of the authors of the monograph should be supplemented on the applicability of this type of tomography for reconstruction of primarily plane objects using only the first method of increasing the information content of testing. Further, the effectiveness of the second method to increase the information content for reconstruction of volumetric local objects of a complex structure will be shown.

2 Experiments and Results

Consider the problem of reconstructing a plane electrically conductive object via scanning the surface of an ECT object with a local zone of interaction between the exciting magnetic field and the test object as an example.

Figure 1 shows a removable ECT over three metal plates located close to each other as a composite object: duralumin plate of (60 × 60 × 1) mm, duralumin plate of (60 × 60 × 2) mm and steel plate of (60 × 60 × 0.3) mm. The upper surfaces of the plates are in the same *XY* plane.

The design parameters of the removable transformer differential ECT used in the experiment were as follows: the diameter of the excitation winding (EW) middle turn was 36 mm; the diameter of the measuring winding (MW) and compensation winding (CW) middle turn was 32 mm; the distance between the planes of the middle turns of the MW and CW located symmetrically relative to the EW was 22 mm. The gap between the ECP and the *XY* plane was 8 mm. The excitation current frequency was 250 Hz.

The eddy current measuring system used in the experiment was based on the IVN-03 applied voltage meter developed in the Laboratory for Electromagnetic Testing, TPU, which enables measuring the amplitudes of the complex components of the ECT applied voltage with a relative error not exceeding ± 1%.

Before the experiment, the initial ECT voltage was automatically compensated for in the absence of the test object. During the experiment, the ECT was moved parallel to the *XY* plane in the range of (−105 to 105) mm along the *Y* axis and in the range of (−45…45) mm along the *X* axis with an increment of 5 mm.

Figure 2 shows the dependences of the amplitude *A** and phase φ of the relative applied voltage of the ECT on the X and Y coordinates. The maximum value of the amplitude *A** was 0.08. The phase variation range was (–19 to 86)°.

The analysis of the obtained results on the interaction of the ECT magnetic field and the composite plane object (the results of direct eddy current transformation) shows that the test object can be reconstructed with a certain degree of reliability (the inverse problem of eddy current transformation has been solved). In particular, the pattern of the dependences in Fig. 2 indicates that the test object consists of three

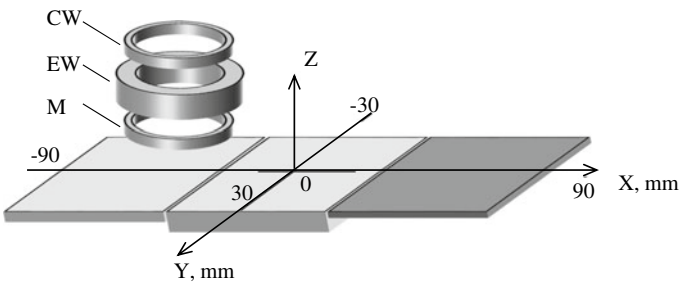

Fig. 1 A removable ECT over a plane composite metal object

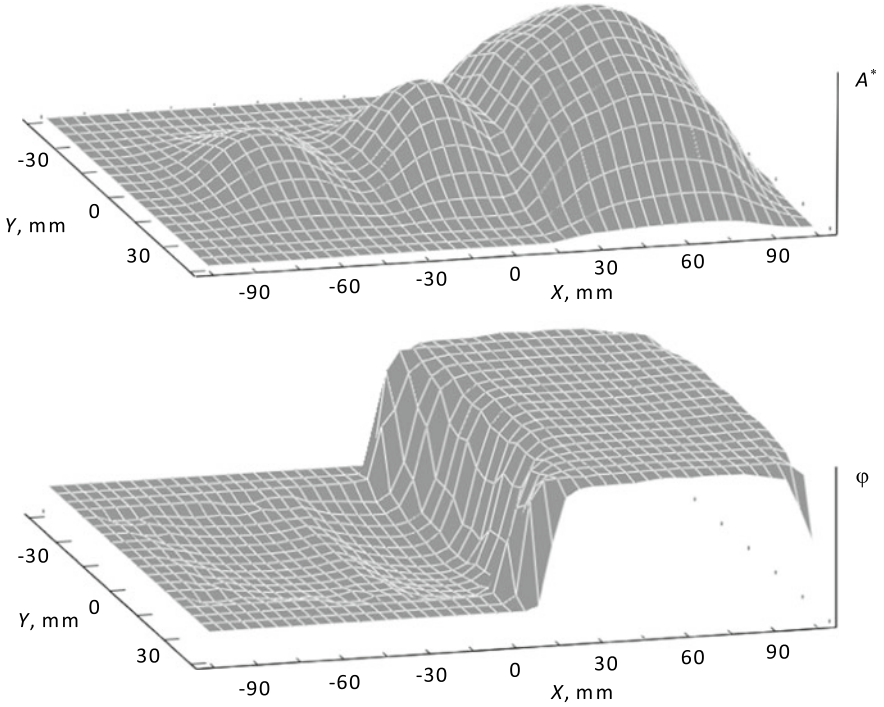

Fig. 2 Dependence of the amplitude A^* and phase φ of the relative applied voltage of the ECT on the X and Y coordinates

plane square-shaped components, two of which are made of non-magnetic material, and one is made of magnetic one. In this case, it can be concluded that, although non-magnetic parts are located relative to each other gapless, they are not one whole.

If necessary, the distance from the ECT to the metal plates and the thickness and electrical conductivity of non-magnetic components can be determined using conventional methods of eddy current testing, for example, the three-frequency method of eddy current testing of non-magnetic metal objects described in [7, 8]. According to this method, the first frequency is selected as a negligibly small value of the penetration depth of the magnetic field in comparison with the plane object thickness. The second frequency is selected from the condition that the penetration depth of the magnetic field is approximately equal to half the thickness of the object The third frequency is selected from the condition that the penetration depth of the magnetic field exceeds the object thickness. In this case, the applied voltage of the ECT at the first frequency depends on the gap h between the transducer and the test object only. The applied voltage at the second frequency depends on the gap h and the specific electrical conductivity σ of the material. The applied voltage at the third frequency depends on the gap h, the specific electrical conductivity σ of the material and the object thickness T.

The h value is determined by the value of the applied voltage amplitude of the first frequency. The values of the complex components of the applied voltage of the second frequency and the calculated gap value are used to determined the σ value. The values of the complex components of the applied voltage of the third frequency and the calculated values of the gap h and the material specific electrical conductivity σ are used to determine the object thickness T. The functions of the inverse transformation obtained in the numerical analysis of the functional dependences of the applied voltages of the ECT on the specified parameters of the object are used to determine the test object parameters: the gap h, the material specific electrical conductivity σ and the object thickness T.

Thus, a detailed reconstruction of the composite test object can be carried out. Moreover, testing can be performed even if there is an electrically conductive shield between the ECT and the test object (reconstruction of a multilayer object).

Figure 3 shows the dependences of the amplitude A^* and phase φ of the relative applied voltage of the ECP on the X and Y coordinates for the object in Fig. 1 in the presence of a duralumin plate 1.2 mm thick located directly above the XY plane. The

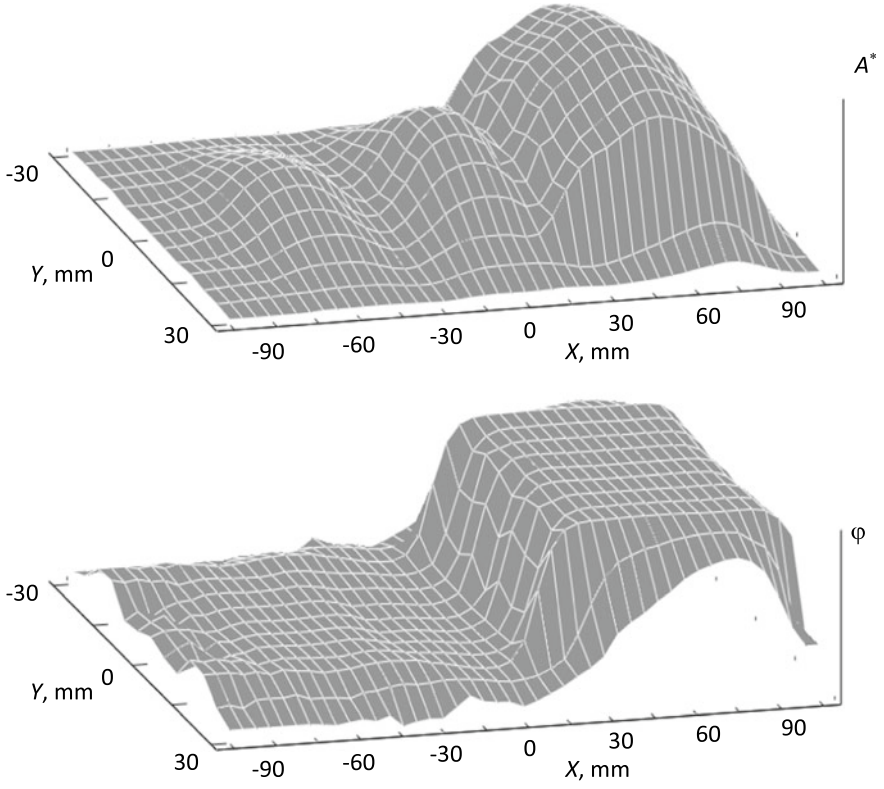

Fig. 3 Dependence of the amplitude A^* and phase φ of the relative applied voltage of the ECT on the X and Y coordinates when using the shield

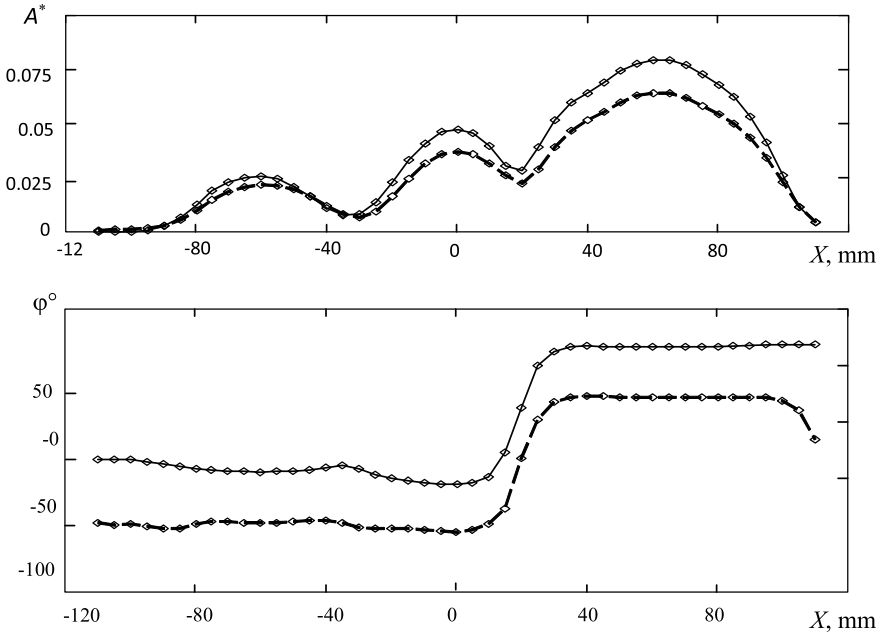

Fig. 4 Dependences of the amplitude A* and phase φ of the relative applied voltage of the ECT on the X coordinate at Y = 0 without (solid line) and with (dashed line) the shield

effect of the shield was minimized by balancing the ECT in the absence of the test object but in the presence of the shield.

The maximum amplitude A^* in this case was 0.065. The phase variation range was (–57 to 48)°.

A comparative analysis of the interaction results for the cases of absence and presence of the shield shows that the results are qualitatively similar. Figure 4 illustrates the quantitative difference between the results. It shows the dependences of the amplitude A^* and phase φ of the relative input voltage of the ECT on the X coordinate at $Y = 0$ for the cases of absence and presence of the shield. The differences in the values of the amplitude and phase are of natural character and can be compensated in the first case by multiplicative corrections, and in the second case by additive ones.

It should be noted that the decreased diameter of the ECT windings can enlarge the test area and, accordingly, provide more data on the properties of an electrically conductive test object. However, in this case, the maximum distance from the ECT to the object reduces.

Another way to increase the information value of eddy current testing and to provide more data on the results of eddy current tomography is measurement at different angles of mutual spatial orientation of the field strength vector of the exciting magnetic field and the test object [9]. As an example, consider the problem of reconstructing volumetric local electrically conductive objects in the form of rotating body for single objects located in the test area, and for pairs of objects with coaxial and

non-coaxial orientation. The appearance and characteristics of the objects are shown in Fig. 5.

Figure 6 illustrates the transformer ECT with a two-section EW $w1$ and MW $w2$ located coaxially with the EW sections and at similar distance from them. The diameter of the middle turn of the windings is 320 mm, and the distance between the

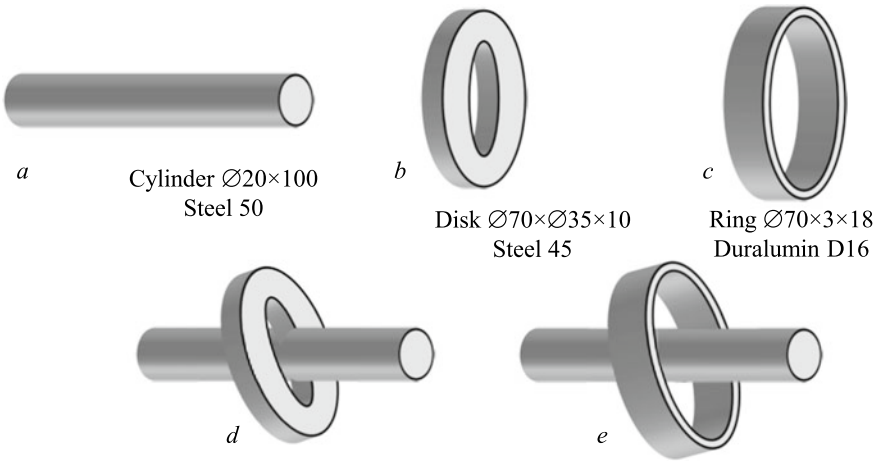

Fig. 5 Volumetric local electrically conductive objects: rotation bodies (**a**–**c**) and their pair combinations in the non-axial orientation (**d**, **e**)

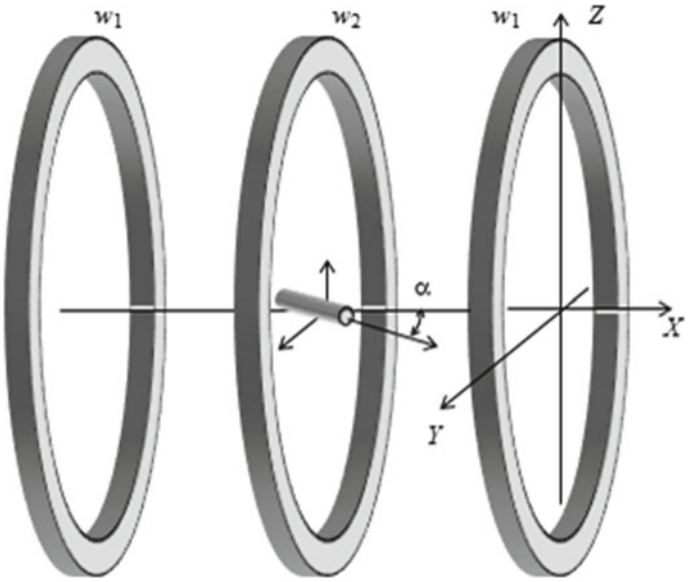

Fig. 6 Electrically conductive object in the ECT test area

windings is 120 mm. This ratio of the ECT geometric parameters in the middle zone of the test area ensures highly uniform sensitivity of the transducer to an electrically conductive object. Thus, when an electrically conductive object of a spherical shape moves within a spherical region with a diameter of 160 mm located in the center of the ECT, the relative change in the applied voltage amplitude does not exceed 5%.

The ECT comprises a special device for rotating the object in the XY plane and fixing the rotation angle α to ensure measurement at different mutual orientations of the exciting magnetic field (directed along the X axis) and the test object. The orientation angle α was changed in the range of (0–180)° with an increment of 15°.

During the experiments, the excitation current frequency was 1 kHz. The amplitudes of the complex components of the applied voltage of the ECT were measured using the previously mentioned IVN-03 meter.

Figure 7 shows the hodographs of the relative applied voltage for changes in the orientation with respect to the force lines of the magnetic field of objects in the form of rotation bodies. Hodographs of $\dot{U}^*_{\text{INS}}$ for changes in the orientation of these objects with respect to the force lines of the ECT magnetic field are straight lines with the ends corresponding to the longitudinal and transverse orientations in the magnetic field.

Thus, the reflection of the parameters of the rotation bodies are two complex values $\dot{A}$ and $\dot{B}$ equal to the values $\dot{U}^*_{\text{INS}}$ for the longitudinal ($\alpha = 0$) and transverse.

($\alpha = 90°$) orientations of the object in the magnetic field, respectively. As shown in [10], modules of complex values $\dot{A}$ and $\dot{B}$ are proportional to the cube of the characteristic size of the test object. These are the size of the object in the corresponding direction of the magnetizing field for ferromagnetic objects and the size of the object in the plane orthogonal to the direction of the magnetizing field for nonmagnetic objects. The ratio of the moduli of $\dot{A}$ and $\dot{B}$ shows the ratio of the longitudinal and transverse dimensions of the object, and the phase values indicate the electromagnetic properties of the material.

Figure 8 shows the hodographs of the relative applied voltage for changes in the orientation relative to the force lines of the magnetic field of pairs of objects in the form of rotation bodies in their coaxial orientation. In this case, the hodographs of $\dot{U}^*_{\text{INS}}$ for changes in the orientation of these composite objects relative to the force lines of the ECT magnetic field are straight lines with the ends corresponding to the longitudinal and transverse orientations in the magnetic field.

Figure 9 shows the hodographs of the relative applied voltage for changes in the orientation with respect to the force lines of the magnetic field of the same pairs of rotation bodies in non-axial orientation (angle β between the direction of the longitudinal axes was set equal to 30°). Hodographs for changes in the orientation of such composite objects with respect to the force lines of the ECT magnetic field are not straight lines but ellipses.

The ratio of the axes of the ellipses shows the degree of non-axiality of the test objects. To illustrate this, we experimentally determined the dependence of the ratio of the axes of the ellipse ε on the angle β for a pair of rotation bodies—a ferromagnetic cylinder and a duralumin ring (Fig. 10). Analysis of this dependence shows that for coaxial ($\beta = 0°$) and orthogonal ($\beta = 90°$) mutual orientation of rotation bodies, the

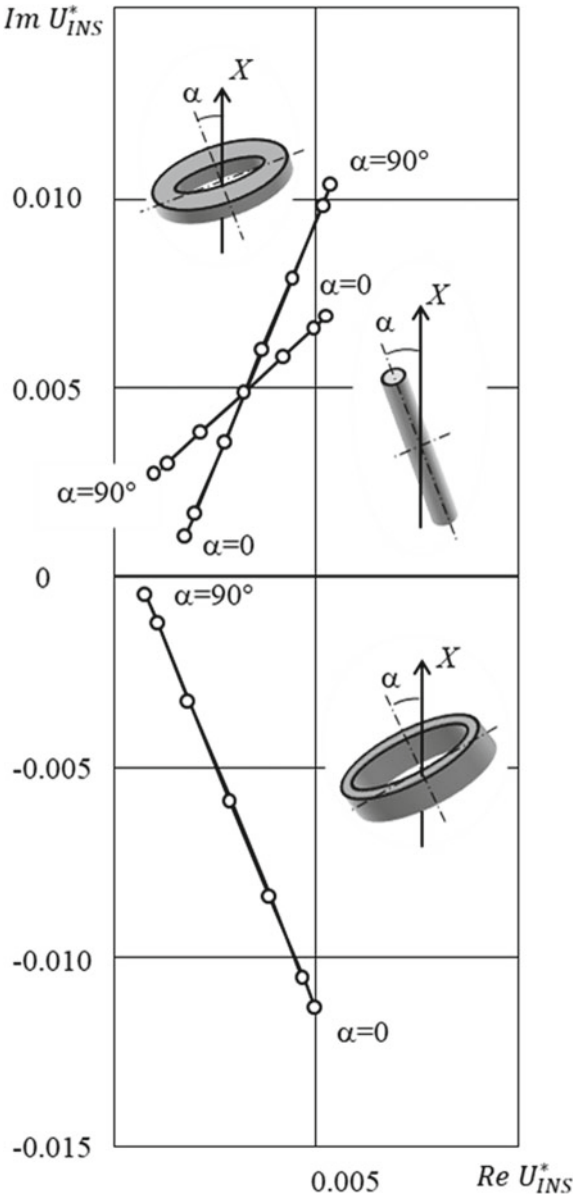

Fig. 7 Hodographs of $\dot{U}^*_{\mathrm{INS}}$ for rotation of the objects in the form of rotation bodies

ratio of the ellipse axes (the minor axis-to large axis length ratio) is zero. When the angle β changes in the range of (0–90)°, the ratio ε for this asymmetric object changes in the range of (0–0.5). The maximum value ε corresponds to the non-axiality angle $\beta \approx 40°$. The ε(β) dependence is almost cosinusoidal one.

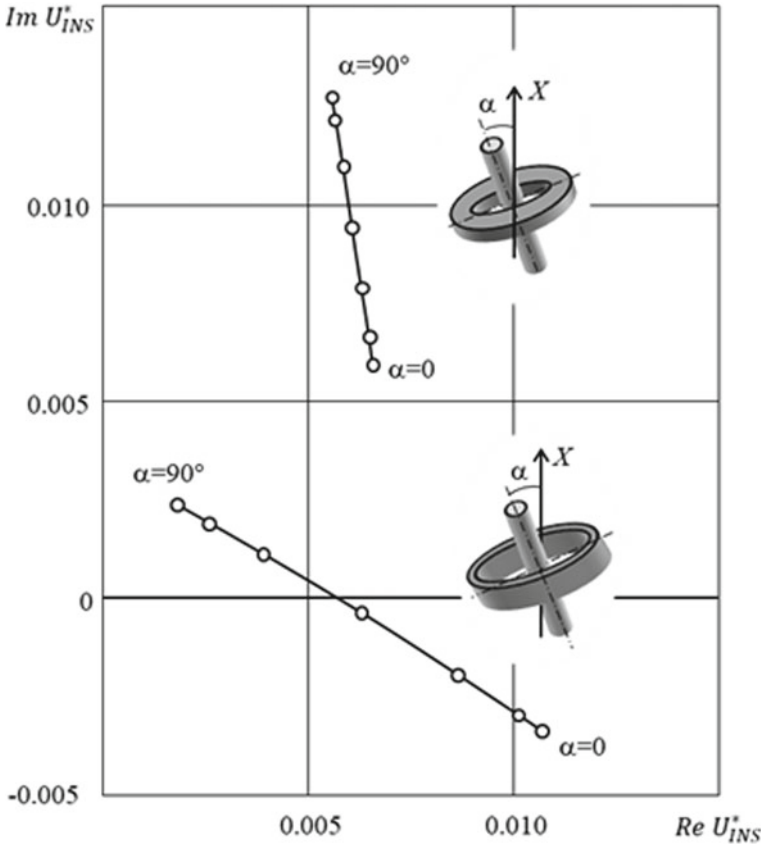

Fig. 8 Hodographs of $\dot{U}^*_{\mathrm{INS}}$ for rotation of the composite objects in the form of rotation bodies in coaxial orientation

Thus, measurements of $\dot{U}^*_{\mathrm{INS}}$ in different mutual orientations of the exciting magnetic field and the test object provide more data on the shape, material, dimensions, and orientation of the electrically conductive object in space. For asymmetric objects, a quantitative assessment of the asymmetry can be carried out.

The described example is a particular case of the orientation of the longitudinal axes of the test objects in the *XY* plane. In the case of arbitrary orientation, the objects should be rotated in at least two orthogonal planes to achieve reliable results of reconstruction.

In addition, practical implementation of the multi-angle interaction of the physical field with the object should be considered. In the first case considered, the ECT was mechanically displaced relative to the plane object, and in the second case, the most local electrically conductive object was mechanically rotated in the ECT magnetic field. However, as shown in [9], electrical methods of scanning objects are more

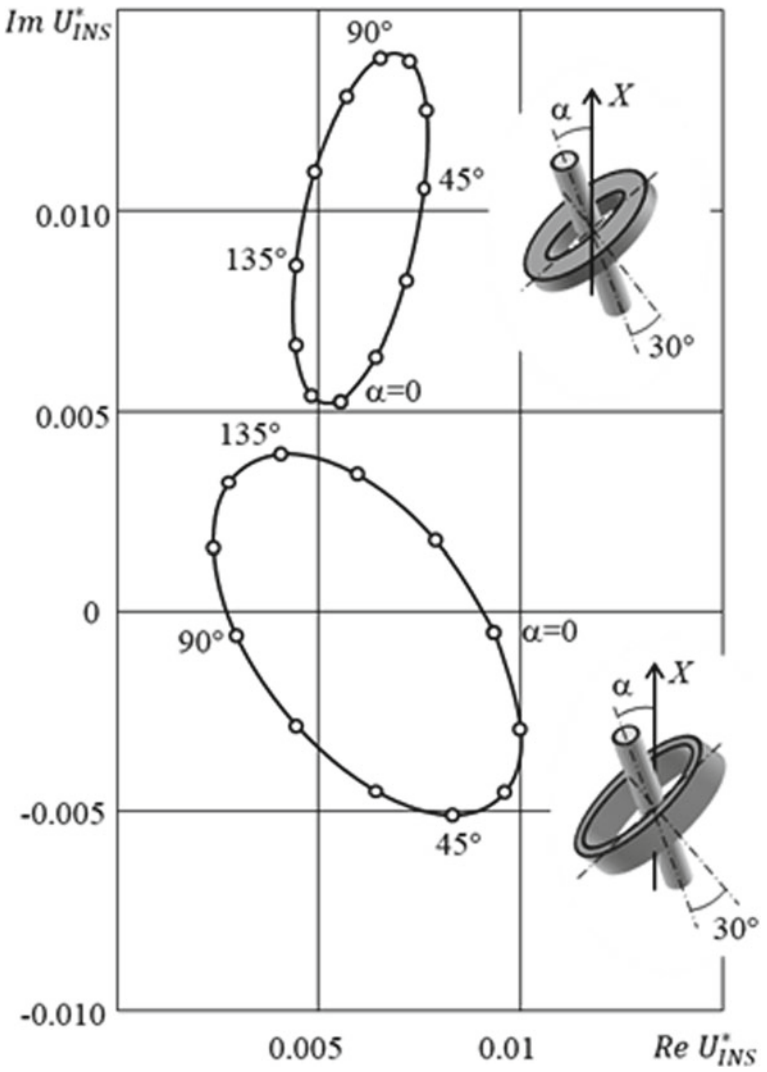

Fig. 9 Hodographs of $\dot{U}^*_{\text{INS}}$ for rotation of the composite objects in the form of rotation bodies in non-axial orientation

suitable due to the appropriate control of the field winding currents and signals of the measuring windings of a multi-winding ECT. These are matrix ECTs [11] and transducers of systems for selective detection of metal objects.

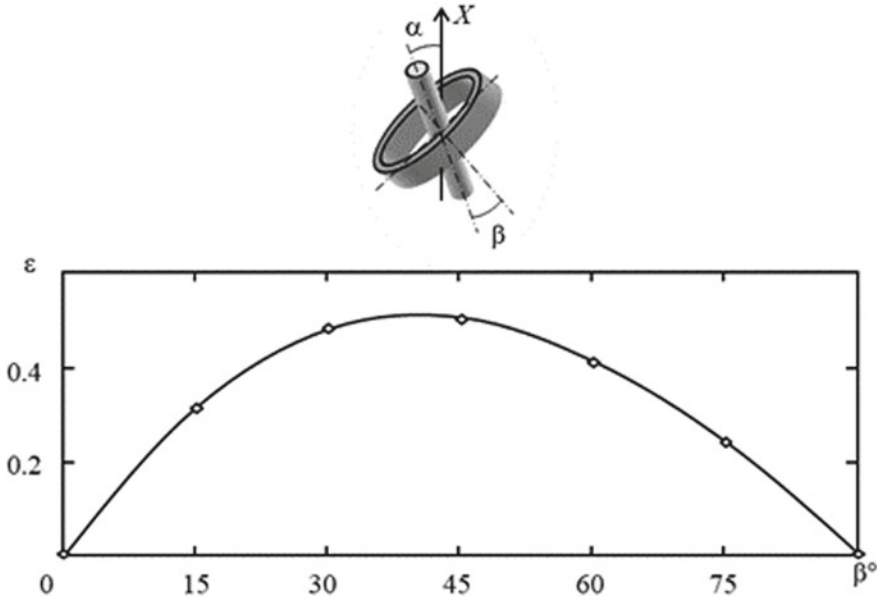

Fig. 10 Dependence of the ratio of the axes of the ellipse ε on the angle β for a pair of rotation bodies—a ferromagnetic cylinder and a duralumin ring

3 Conclusion

Thus, eddy current testing methods can be effectively used to solve a number of technical tomography problems associated with obtaining detailed information about the structure of composite metal objects.

The reconstruction of complex objects can be carried out based on the results of eddy current testing using two methods for increasing the information content of testing. The first method implies scanning the object surface when detecting the interaction zone of the exciting magnetic field of the ECT and the test object, and can be used for monitoring mainly plane electrically conductive objects. The second method provides measurement information at different angles of mutual spatial orientation of the excitation magnetic field strength vector and the test object, and can be used for reconstruction of volumetric local electrically conductive objects.

In the first case, information about the shape, material, dimensions, and continuity of the parts of a plane metal object can be obtained. In the second case, the shape, material, size, and space orientation of an electrically conductive object can be determined. For asymmetric objects, quantitative information can be obtained on the degree of their asymmetry, which can be used, in particular, to control the relative position of the parts.

References

1. Fuchs, T., Keßling, P., Firsching, M., Nachtrab, F., Scholz, G.: Industrial applications of dual X-ray energy computed tomography (2X-CT). RILEM Bookseries **6**, 97–103 (2012). https://doi.org/10.1007/978-94-007-0723-8_13
2. Wang, Z.-B., Shi, G.-H., He, Y., Ding, Z.-H., Zhang, Y.-D.: Application of optical coherence tomography to distance measurement of optical surface. Guangxue Jingmi Gongcheng/Opt. Precision Eng. **20**(7), 1469–1474 (2012). https://doi.org/10.3788/OPE.20122007.1469
3. Barkhatov, V.A.: Development of methods of ultrasonic nondestructive testing of welded joints. Russ. J. Nondestruct. Test **39**(1), 23–47 (2003). https://doi.org/10.1023/A:1024588920109
4. Monte, L., Erricolo, D., Ansari, R., et al: Underground imaging using RF tomography: the effect of lateral waves. In: Proceeding of the 2009 International Conference on Electromagnetics in Advanced Applications, pp. 873–876 (2009). https://doi.org/10.1109/ICEAA.2009.5297354
5. Minin, O.V., et al.: Ultra-wideband radio tomographic imaging with resolution near the diffraction limit. Opt. Quant. Electron. **49**(10), 339 (2017). https://doi.org/10.1007/s11082-017-1172-7
6. Bray, C.L., Hornak, J.P.: Unilateral MRI using a rastered projection. J. Magn. Reson. **188**(1), 151–159 (2007). https://doi.org/10.1016/j.jmr.2007.06.010
7. Tajima, N., Yusa, N., Hashizume, H.: Low frequency eddy current testing to measure thickness of double layer plates made of nonmagnetic steel. Stud. Appl. Electromagn. Mech. **42**, 131–138 (2017). https://doi.org/10.3233/978-1-61499-767-2-131
8. Yakimov, E.V., Urazbekov, E.I., Goldshtein, A.E., Bulgakov, V.F.: Computational transformation of signals of a measuring information system for eddy-current flaw detection. Russ. J. Nondestruct. Test **49**(11), 657–663 (2013). https://doi.org/10.1134/S1061830913110107
9. Goldstein, A.E., Belyankov, V.Y.: An eddy-current gauge for measuring the wall thickness of light-alloy drill pipes. Russ. J. Nondestruct. Test **53**(8), 588–595 (2017). https://doi.org/10.1134/S1061830917080022
10. Ammari, H., Chen, J., Chen, Z., Garnier, J., Volkov, D.: Target detection and characterization from electromagnetic induction data. J. des Mathematiques Pures et Appliquees **101**(1), 54–75 (2014). https://doi.org/10.1016/j.matpur.2013.05.002
11. Chady, T.: A family of matrix type sensors for detection of slight flaws in conducting plates. IEEE Trans. Magn. **35**(5), 3655–3657 (1999). https://doi.org/10.1109/20.800621